Proton-Transfer Tautomerism of 7-Hydroxyquinolines Mediated by Hydrogen-Bonded Complexes

Pi-Tai Chou,*,† Chin-Yen Wei,† Churng-Ren Chris Wang,† Fa-Tsai Hung,‡ and Chen-Pin Chang§

Department of Chemistry, The National Chung-Cheng University, Chia Yi, Taiwan, R.O.C., The National Hu-Wei Institute of Technology, Yunlin, Taiwan, R.O.C., and Department of Chemistry, Fu Jen Catholic University, Shin Chuang, Taiwan, R.O.C.

Received: July 28, 1998; In Final Form: January 19, 1999

The enol−keto proton-transfer tautomerism of 7-hydroxyquinoline (7HQ) mediated by hydrogen-bond formation has been studied in the ground as well as in the excited state. Thermodynamics of self-association and hydrogen-bonded complexes of 7HQ in various nonpolar solvents was obtained by means of absorption, emission, and theoretical approaches. Specific hydrogen-bonding sites in the complex were determined by applying various derivatives of 7HQ incorporated with guest molecules possessing only either a proton-donating or -accepting site. The result can be qualitatively rationalized by a correlation of the hydrogen-bonding strength with respect to the donor's acidity and/or acceptor's basicity. In benzene, the 7HQ cyclic dimer undergoes a fast excited-state double proton-transfer reaction, resulting in a unique keto-tautomer emission. Surprisingly, however, the 1:1 7HQ(enol)/acetic acid complex possessing only a single hydrogen bond undergoes an excited-state double proton-transfer reaction, forming a keto/acid complex. As a result, a proton-transfer mechanism incorporating the rotational diffusion dynamics of guest molecules, i.e., acetic acid, is proposed.

Introduction

Recently, we have studied the enol/keto proton-transfer tautomerism of 7-azaindole (7AI),[1,2] 2-hydroxypyridine,[3] and 3-hydroxyisoquinoline (3HIQ)[4] mediated either by self-association or by adding guest molecules, forming conjugated dual hydrogen-bond (CDHB) complexes. A prototype example can be illustrated in the case of 1:1 3HIQ/acetic acid CDHB complex in cyclohexane (Scheme 1). The dual hydrogen-bonding sites, i.e., the hydroxyl proton and the nitrogen atom in 3HIQ, resonantly induce a π electron charge transfer from the hydroxyl oxygen to the pyridinal nitrogen, resulting in an additional stabilization energy for the hydrogen-bonding formation. Thus, although 3HIQ exists predominantly as an enol monomer in the diluted cyclohexane solution, the enol−keto equilibrium can be fine-tuned by adding guest molecules possessing the bifunctional hydrogen-bonding property.[4] The results in combination with its excited-state proton-transfer dynamics establish a mechanism for the CDHB mediating proton-transfer reaction, which is believed to be crucial if the proton-transfer tautomerism, as proposed, is a key step to induce mutation.[5−7]

In this study, we have extended our investigation to other types of hydrogen-bonding systems in which 7-hydroxyquinoline (7HQ, Figure 1) is a prototype. In aprotic solvents 7HQ exists predominantly as an enol form which possesses a proton donor (the hydroxyl proton) and a proton acceptor (the quinolinic nitrogen) far away from each other (4.748 Å calculated by 6-31G(d,p) basis set, see Figure 8a). Thus, unlike 7AI (or 3HIQ) dimer and/or hydrogen-bonded complexes where CDHB is normally incorporated, the formation of a 1:1 7HQ/guest hydrogen-bonded complex, if it exists, may involve only a single hydrogen bond even though the guest molecule, e.g., acetic acid, possesses the bifunctional hydrogen-bonding property. Multiple hydrogen-bonding formation may also be possible when forming

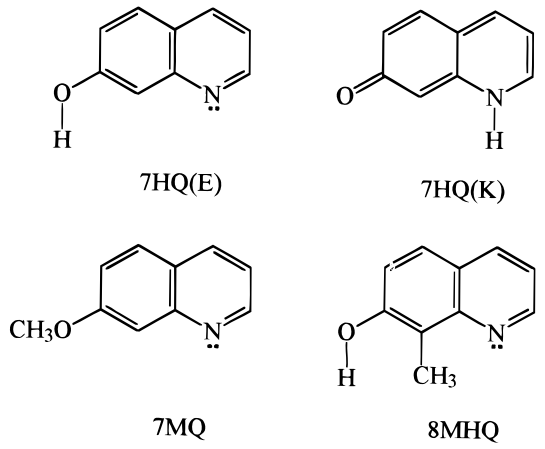

Figure 1. Structures of the proton-transfer isomers and derivatives of 7HQ.

SCHEME 1

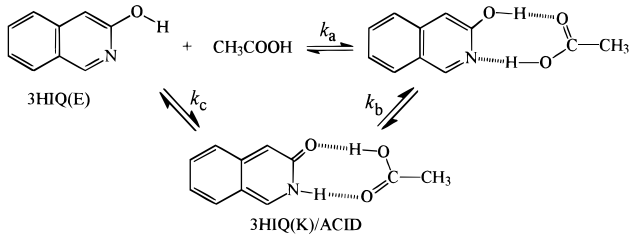

* Author to whom correspondence should be addressed.
† The National Chung-Cheng University.
‡ The National Hu-Wei Institute of Technology.
§ Fu Jen Catholic University.

10.1021/jp983201m CCC: $18.00
Published on Web 03/17/1999

higher-order 1:*n* ($n \geq 2$) 7HQ/guest complexes, which, however, may have an unfavorable entropy factor because they require a larger number of stoichiometric guest molecules for the complexation (vide infra). Previous fluorescence studies have revealed that in a sufficiently low concentration 7HQ exhibits predominantly a normal Stokes shifted emission ($\lambda_{max} \sim 350$ nm) in nonpolar solvents. In contrast, dual emission was observed in methanol, resulting from the normal (the enol form, $\lambda_{max} \sim 380$ nm) and proton-transfer tautomer (the keto form, $\lambda_{max} \sim 520$ nm) species.[8−13] Both steady-state absorption and fluorescence titration studies have drawn the conclusion that the increase of the proton-transfer keto-tautomer emission is associated with the formation of a 1:2 7HQ/methanol complex. On the basis of a nano-picosecond time-resolved study, the rate of excited-state proton transfer for the 1:2 7HQ/methanol complex was measured to be $\sim 5.0 \times 10^9$ s^{-1} at room temperature, and a precursor with a cyclic dual hydrogen-bonding configuration is required prior to the proton-transfer reaction. The barrier height for the ESDPT was estimated to be 0.54 kcal/mol,[11] and the overall proton-transfer mechanism may correlate, in part, with the solvent (i.e., methanol molecules attached to two hydrogen-bonding sites) reorganization energy.[12] Other nonspecifically solvated 7HQ molecules do not undergo proton transfer within the life span of the excited state, resulting in a normal Stokes shifted emission. Perhaps the strongest support for the dual methanol catalyzing double proton-transfer reaction was given by a recent study of the 7HQ derivative, 8-methyl-7-hydroxyquinoline (8MHQ, Figure 1) in which a dual-methanol relay incorporated in the 7HQ/methanol complex is interrupted due to the steric hindrance introduced by the 8-methyl group, prohibiting the double proton-transfer reaction.[14] In this study we have attempted to use 7HQ and its derivatives as a prototype to differentiate between CDHB and single-hydrogen-bonding complexes. Our goal is to further explore the role of the hydrogen-bond formation contribution to the proton-transfer tautomerism in the ground as well as in the excited state.

The following sections are organized according to a sequence of steps where we first performed absorption titration experiments to determine the equilibrium constants for various 7HQ hydrogen-bonded complexes in nonpolar solvents. The next step involved steady-state and time-resolved fluorescence measurements to examine the excited-state proton-transfer properties. We have determined specific hydrogen-bonding sites in the complex by applying various derivatives of 7HQ incorporated with guest molecules possessing only either a proton-donating or -accepting group. Finally, attempts have also been made to rationalize the results by a theoretical approach in which a correlation between the hydrogen-bonding site with respect to donor acidity (pK_a) and acceptor basicity (pK_b) will be established.

Experimental Section

Material. 7HQ (Aldrich) was purified by column chromatography (eluent 1:3 *n*-hexane: ethyl acetate) followed by recrystallization twice from acetonitrile. 7MQ was synthesized by two different methods. In a conventional approach a 1:1 equivalent 7HQ:dimethyl sulfate was refluxed in CH_2Cl_2 to obtain 7MQ. However, such a method gives rise to a side product difficult to separate from 7MQ, which also exhibits strong fluorescence interference in the region of interest. Alternatively, this obstacle can be overcome by using diazomethane instead of dimethyl sulfate followed by column chromatography (20:1(v/v) CH_2Cl_2:ethyl acetate) to obtain the impurity-free 7MQ. 8-Methyl-7-hydroxyquinoline (8MHQ) was synthesized by the reaction of 3-amino-*o*-cresol and acrolein in the acidic condition using a standard Skraup method.[15] The final product was purified by column chromatography (eluent 1:3 hexanes:ethyl acetate) followed by recrystallization from acetonitrile. Acetic acid (ACID, Merck Inc.) and 2-azacyclohexanone (ACH, Aldrich) were purified according to the previously described method.[4] CCl_4 (Merck Inc.) was used without further purification because no interference due to impurity fluorescence was detected in the wavelength region of interest. Benzene and cyclohexane (Merck Inc.) were of spectragrade quality and were refluxed several hours over calcium hydride under a nitrogen atmosphere and were transferred, prior to use, through distillation to the sample cell.

Measurements. Steady-state absorption and emission spectra were recorded by a Cary 3E (Perkin−Elmer) spectrophotometer and a Hitachi (SF4500) fluorimeter, respectively. Both wavelength-dependent excitation and emission response of the fluorimeter have been calibrated according to a previously reported method.[4] Nanosecond lifetime measurements were performed by an Edinburgh FL 900 photon counting system with a hydrogen-filled flash lamp/or a nitrogen lamp as the excitation source. The temporal resolution after deconvolution of the excitation pulse was ~200 ps. The data were analyzed using a nonlinear least-squares fitting program with a deconvolution method reported previously.[16]

Theoretical Calculations. The initially optimized structure used for the ab initio calculation was obtained by the semiempirical AM1 method using a Spartan package (Release 3.1.6, Wavefunction, Inc., Irvine, 1994). Ab initio molecular orbital calculations were performed by using Gaussian 94 Rev D.3 programs. Geometry optimizations for all structures were carried out with the 6-31G(d,p) basis set at the Hartree−Fock (HF) level. This basis set has proven to be suitable for the dimer (or complex) formation incorporating hydrogen-bond formation.[17] Hessians, and hence vibrational frequencies, were also performed to check whether the optimized geometrical structure for those dimeric and complex forms is at an energy minimum, transition state, or higher-order saddle point. The directly calculated zero-point vibrational energies (ZPE) were scaled by 0.9181[18] to account for the overestimation of vibrational frequencies at the HF level. The association energy, ΔH_{ac}, was calculated as the change in the total molecular enthalpy of formation in the conversion of the optimized monomer individually into the optimized dimer or complex.

The following sections are organized according to a sequence of steps where we first performed detailed absorption and fluorescence titration experiments to determine the thermodynamic properties of hydrogen-bonded complexes for 7HQ and its derivatives. The results lead us to deduce specific hydrogen-bonding sites in the 7HQ/guest complexes. Subsequently, an ab initio calculation was carried out to provide complementary support for the structure of the 7HQ/guest hydrogen-bonded complexes. Finally, plausible mechanisms for the excited-state proton-transfer reaction are proposed and discussed.

Results

Ground-State Equilibrium. *7HQ Self-Association*. Due to the sparse solubility in nonpolar hydrocarbon solvents (e.g., cyclohexane), studies of self-association for 7HQ were carried out in benzene solution. However, since the theoretical approach in a later section simulates the gas-phase condition, to have a fair comparison, studies of other 7HQ hydrogen-bonded complexes only requiring sufficiently low concentration of 7HQ have

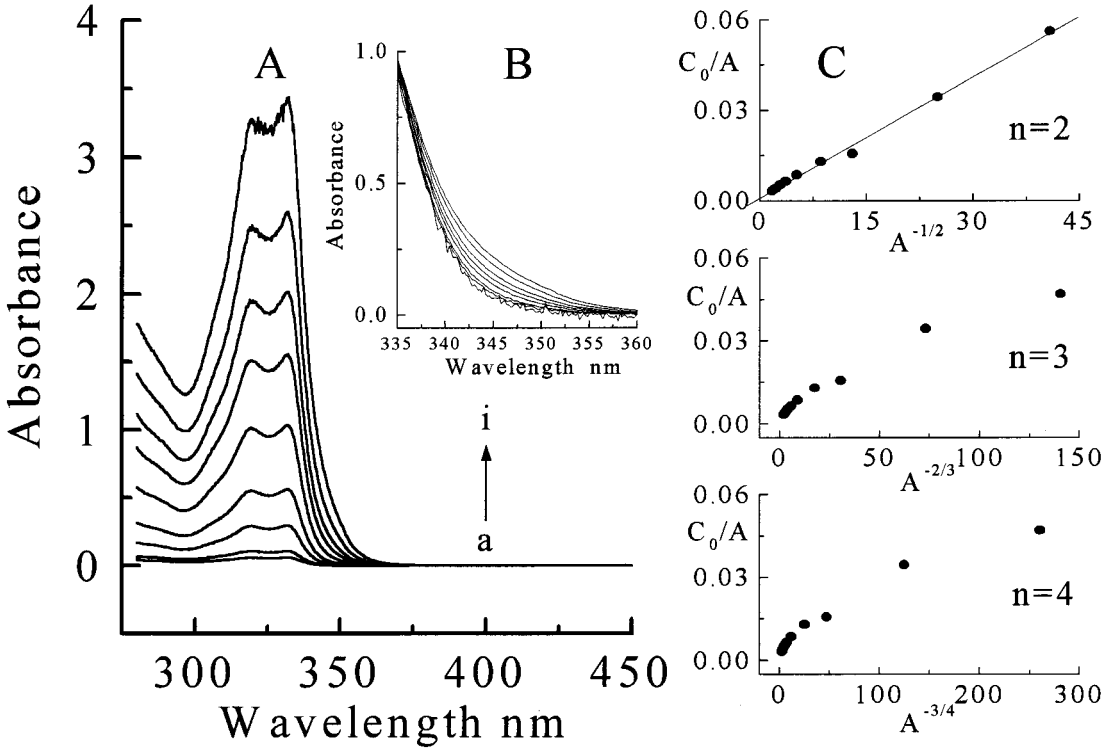

Figure 2. (A) The concentration-dependent absorption spectra of 7HQ in benzene, in which 7HQ was prepared at (a) 1.82×10^{-5}, (b) 3.37×10^{-5}, (c) 9.26×10^{-5}, (d) 1.76×10^{-4}, (e) 3.22×10^{-4}, (f) 4.87×10^{-4}, (g) 6.27×10^{-4}, (h) 8.14×10^{-4}, and (i) 1.08×10^{-3} M. (B) The absorption spectra in the region of 330−360 nm by normalizing concentration-dependent spectra shown in A. (C) Plot of C_0/A_{350} against $n\sqrt{1/A_{350}^{n-1}}$ with $n = 2$ to 4. For the $n = 1$ plot, a linear best least-squares fitted curve (solid line) is also shown.

also been performed in CCl_4 and cyclohexane. Figure 2A shows the concentration-dependent absorption spectra of 7HQ in benzene. When the concentration was as low as 7.0×10^{-6} M in benzene, 7HQ exhibits a S_0-S_1 absorption band maximum at ∼332 nm. Upon increasing the concentration, a previously unrecognized spectral feature appears as a shoulder in the region of > 340 nm (see Figure 2B). In comparison, 7MQ is generally treated as an enol model in which the enol−keto tautomerism is prohibited due to its lack of a hydroxyl proton. Furthermore, the lack of the hydroxyl proton also prevents the formation of any hydrogen-bonded self-aggregation. The results show a structural, concentration-independent S_0-S_1 absorption maximum at ∼330 nm (see Figure 4a), for which the spectral features are similar to that of 7HQ when the concentration was prepared as low as 7.0×10^{-6} M. We thus conclude that at a sufficiently low concentration, 7HQ exists mainly as the enol monomer form. (Hereafter, 7HQ denotes the enol form of 7-hydroxyquinoline). Upon increasing concentration, the 7HQ dimer and/or higher-order aggregates gradually appear, resulting in a spectral red-shift with respect to the 7HQ monomer. However, unlike the self-association of 3HIQ in which the CDHB effect induces the enol → keto tautomerism in the ground state,[4] at the highest concentration prepared (1.08×10^{-3} M) no detectable absorbance attributed to the S_0-S_1 transition of 7HQ keto tautomer (400−500 nm, vide infra) was observed.

A competitive equilibrium between the enol monomer and 7HQ self-association incorporating n 7HQ molecules can be depicted as $n(7HQ) \rightleftharpoons (7HQ)_n$. Consequently, the association constant K_a for the formation of the $(7HQ)_n$ complex can be expressed as

$$K_a = \frac{C_p}{(C_0 - nC_p)^n} \tag{1}$$

where C_0 is the initial concentration of 7HQ, and C_p denotes the concentration of the 7HQ self-association form. Since at sufficiently long wavelengths, e.g., 350 nm, the absorption can be mainly attributed to the 7HQ self-association, one can incorporate the Beers−Lambert law and write

$$A_{350} = \epsilon_{350} C_p l \tag{2}$$

where A_{350} and ϵ_{350} are the absorbance and the molar extinction coefficient of the 7HQ hydrogen-bonded form at 350 nm, and l is the path length of the cell. When C_p is relatively smaller than C_0, combining eqs 1 and 2 leads to eq 3:

$$\frac{C_0}{A_{350}} = n\sqrt{\frac{1}{\epsilon_{350} K_a l}}\, n\sqrt{\frac{1}{A_{350}^{n-1}}} + \frac{n}{\epsilon_{350} l} \tag{3}$$

For the case of $n = 2$, plotting C_0/A_{350} versus the square root of $1/A_{350}$ (see Figure 2C) gives sufficiently linear behavior in the range of the concentration studied ($1.80 \times 10^{-5}-1.08 \times 10^{-3}$ M). We also must consider the possibility of forming higher-order 7HQ aggregates. As shown in Figure 2C, plotting C_0/A_{350} against $n\sqrt{1/A_{350}^{n-1}}$ for $n = 3$ and 4 deviates from the linearity significantly. It should be noted that eq 3 is derived under the assumption of only one hydrogen-bonded species existing in the equilibrium. At this stage we have no definitive evidence to eliminate the possibility of the coexistence of various types of 7HQ aggregates in the solution. However, the correlation coefficient of 0.992 fitted by $n = 2$ seems to substantially support the dominant $2(7HQ) \rightleftharpoons (7HQ)_2$ equilibrium in benzene, i.e., a 7HQ dimeric species prevailing over other higher-order aggregates. The best least-squares fit for $n = 2$ gives a K_a value of 1.2×10^3 M^{-1}, corresponding to a $\Delta G°$ value of −4.2 kcal/mol at room temperature. An attempt to measure K_a as a function

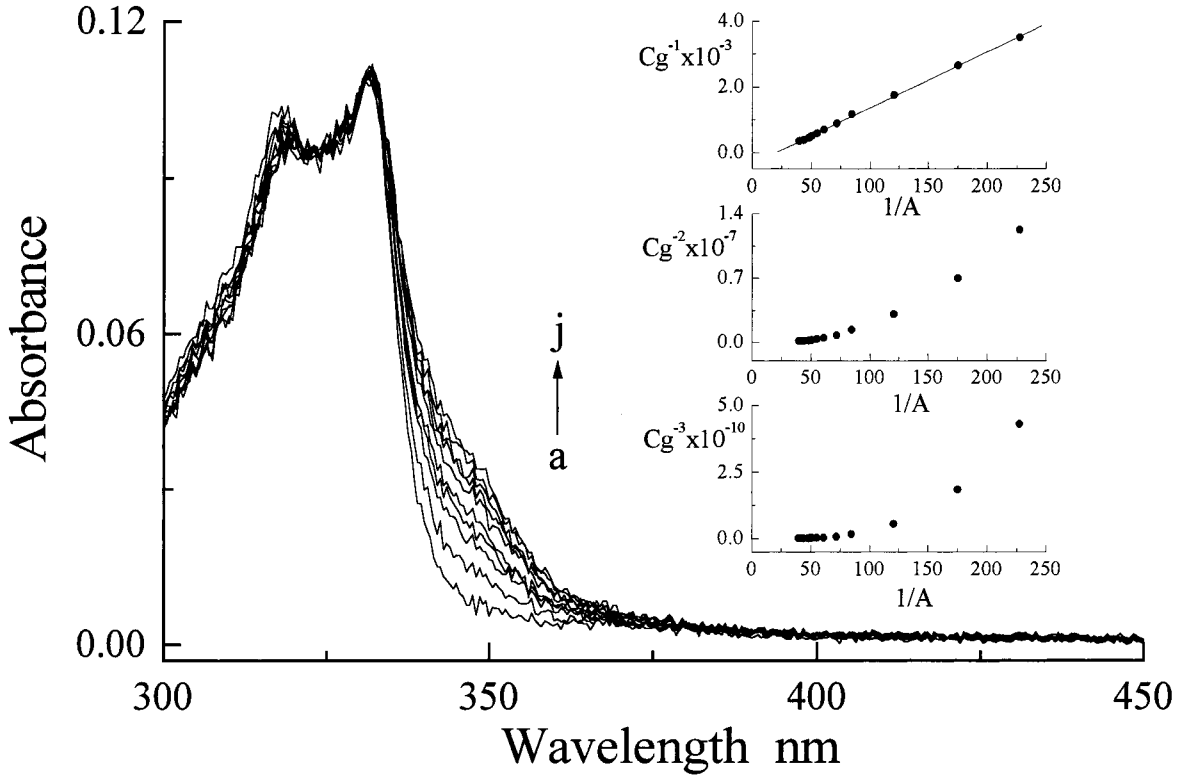

Figure 3. The concentration-dependent absorption spectra of 7HQ (1.1×10^{-5} M) in CCl_4 by adding various ACID concentrations (C_g) of (a) 0, (b) 2.9×10^{-4}, (c) 5.7×10^{-4}, (d) 8.6×10^{-4}, (e) 1.1×10^{-3}, (f) 1.4×10^{-3}, (g) 2.0×10^{-3}, (h) 2.3×10^{-3}, (i) 2.6×10^{-3}, and (j) 2.9×10^{-3} M. Insert: the plot of $1/c_g^n$ against $1/A_{350}$ up to $n = 3$.

of temperature in order to extract the enthalpy of the association, ΔH_{ac}, unfortunately failed due to the sparse solubility of 7HQ at low temperature. Nevertheless, a detailed discussion of ΔH_{ac} based on a theoretical approach and its correlation with respect to the hydrogen-bonding strength will be presented in the section on theoretical calculations.

7HQ/Guest Hydrogen-Bonded Complexes. Figure 3 shows the absorption spectra of 7HQ upon adding the acetic acid in CCl_4. In this experiment, the initial concentration of 7HQ, C_0, was prepared to be as low as 1.0×10^{-5} M to avoid self-dimerization. The formation of 7HQ/ACID hydrogen-bonded complexes can be clearly indicated by the growth of a ~350 nm shoulder throughout the titration. The 7HQ hydrogen-bonded complex incorporating stoichiometric n ACID molecules can be depicted as

$$7HQ + n\text{ACID} \rightleftharpoons 7HQ/(\text{ACID})_n$$

Similarly, the absorbance peak at 350 nm can be exclusively attributed to the S_0-S_1 transition of the hydrogen-bonded complex 7HQ/$(\text{ACID})_n$. Neglecting the steric effect it is reasonable to assume n to be ≤ 4 since each 7HQ may accommodate as many as four hydrogen-bonding sites. On the basis of the Benesi−Hildebrand derivation,[19] the relationship between the initially prepared ACID concentration, C_g, and the measured absorbance at 350 nm, A_{350}, can be expressed in eq 4:

$$\frac{1}{C_g^n} = C_0 \epsilon_{350} K_a \frac{1}{A_{350}} - K_a \qquad (4)$$

The insert of Figure 3 shows the plot of $1/C_g^n$ against $1/A_{350}$ up to $n = 3$ for the experimental data. The results clearly indicate a linear behavior for the $n = 1$ plot. Just as the higher-order self-association of 7HQ must be considered, the coexistence among 7HQ/ACID, 7HQ/$(\text{ACID})_2$, and 7HQ/$(\text{ACID})_3$ complexes in the equilibria is possible and cannot be ruled out in this study. However, a correlation coefficient of 0.996 applying the best least-squares fit to the $n = 1$ plot indicates that even with the formation of higher-order 7HQ/$(\text{ACID})_n$ ($n \geq 2$) complexes, the amount present should be negligibly small within the range of concentration studied. This viewpoint will be further supported in the section on the fluorescence titration experiment. The intercept of the $n = 1$ plot gives a K_a value of 3.5×10^2 M^{-1} in CCl_4, corresponding to a $\Delta G°$ value of −3.5 kcal/mol at room temperature. Similar 7HQ/ACID hydrogen-bonding complexation was observed in cyclohexane, and a K_a value was determined to be 7.8×10^2 M^{-1}. For the case of using 2-azacyclohexanone (ACH) as the guest molecule, the $n = 1$ plot using eq 4 for the experimental results also exhibits a linear behavior, indicating the formation of a 1:1 7HQ/ACH hydrogen-bonded complex. The best-fit gives a K_a value of 4.2×10^2 M^{-1} in CCl_4. Applying a sufficiently low 7HQ concentration (7.0×10^{-6} M) we were able to perform a temperature-dependent study for both 7HQ/ACID and 7HQ/ACH complexes in CCl_4 from 10° to 35 °C, and ΔH_{ac} was calculated to be −7.2 and −6.1 kcal/mol, respectively. Thermodynamic data of 7HQ hydrogen-bonded complexes in other solvents were also obtained and the results are listed in Table 1.

Unlike 7AI and 3HIQ where the CDHB effect plays a crucial role to further stabilize the complex formation, the far separation between hydroxyl proton and the quinolinic nitrogen in 7HQ leads to a 1:1 cyclic dual hydrogen-bond formation virtually impossible for the cases of 1:1 7HQ/ACID and 1:1 7HQ/ACH complexes. Accordingly, both complexes should incorporate only a single hydrogen-bond formation. This viewpoint can be supported by the measured K_a value of 7.8×10^2 M^{-1} for the 7HQ/ACID complex in cyclohexane (see Table 1), which is

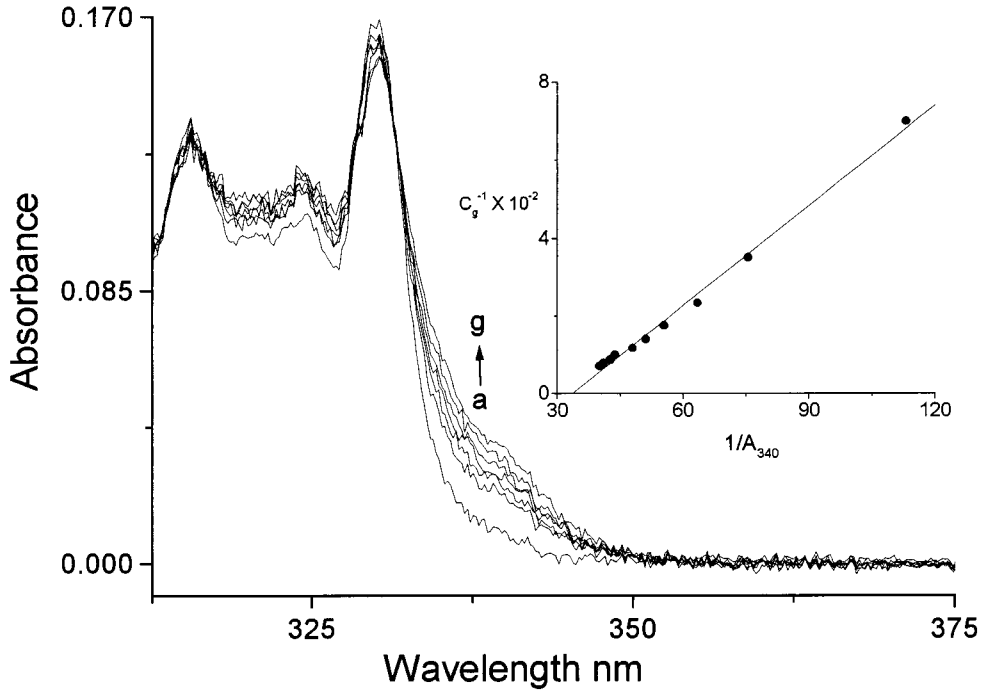

Figure 4. The concentration-dependent absorption spectra of 7MQ (7.8×10^{-6} M) in CCl_4 by adding various ACID concentrations (C_g) of (a) 0, (b) 1.43×10^{-3}, (c) 2.86×10^{-3}, (d) 4.29×10^{-3}, (e) 7.14×10^{-3}, (f) 8.57×10^{-3}, and (g) 1.43×10^{-2} M. Insert: the plot of $1/c_g^n$ against $1/A_{350}$ for $n = 1$.

TABLE 1: Thermodynamic Properties of 7HQ and 7MQ Hydrogen−Bonded Species in Various Solvents

host	guest	solvents	$K_a \times 10^{-2}$ M^{-1} (absorption)	$K_a \times 10^{-2}$ M^{-1} (emission)	ΔH^a (kcal/mol)
7HQ	7HQ	benzene	12		*b*
7HQ	ACID	cyclohexane	7.8	6.8	*b*
7HQ	ACID	CCl_4	3.5	3.3	−7.2
7HQ	ACH	cyclohexane	8.7	3.9	*b*
7HQ	ACH	CCl_4	4.2	*c*	−6.1
7MQ	ACID	cyclohexane	5.2	*c*	
7MQ	ACID	CCl_4	2.9	*c*	
7MQ	ACH	cyclohexane	*d*		
7MQ	ACH	CCl_4	*d*		

[a] ΔH was obtained through a temperature-dependent absorption study of K_a value from 313−283 K. [b] Data were not obtainable due to the sparse solubility of 7HQ at low temperature. [c] The emission is too weak to perform the concentration-dependent study. [d] Negligible change of the absorption spectra even though the concentration of the guest molecule increases up to 2×10^{-3} M.

less than that of 7AI/ACID and 3HIQ/ACID CDHB complexes by a factor of more than twenty.[1−4] Since 7HQ possesses both proton-donating and -accepting sites, it is thus intriguing to know which functional group, the hydroxyl hydrogen or the quinolinic nitrogen atom, acts as an active hydrogen-bonding site. Such a key question unfortunately cannot be unambiguously resolved because the guest molecules also possess bifunctional hydrogen-bonding properties. One way to overcome such an obstacle is to reduce the number of hydrogen-bonding sites in 7HQ. Accordingly, an absorption titration study was also performed in 7MQ. Due to the lack of hydroxyl proton and weak proton-accepting capability of the methoxyl oxygen it is reasonable to predict that the hydrogen-bond formation for the 7MQ hydrogen-bonded complex, once formed, must be at the quinolinic nitrogen site. As shown in Figure 4, 7MQ exhibits a concentration-dependent absorption spectral evolution throughout the titration by acetic acid. The plot of $1/C_g$ against $1/A_{340}$ exhibits linear behavior, and a best least-squares fit gives a K_a value of 2.9×10^2 and 5.2×10^2 M^{-1} in CCl_4 and cyclohexane, respectively. The results of similar spectral and thermodynamic properties between 7HQ/ACID and 7MQ/ACID complexes lead us to conclude that in 7HQ it is more appropriate to assign the hydrogen-bonding site to the quinolinic nitrogen, forming a hydrogen bond with the carboxylic hydrogen.

Surprisingly, in contrast, the formation of the 7MQ/ACH complex was not detected upon increasing the ACH to 2×10^{-3} M. The result clearly implies that the specific type of hydrogen bond incorporated in 7HQ/ACH and 7MQ/ACH, if formed, may be quite different. The quinolinic nitrogen, which is the only active site in 7MQ, is apparently not involved in the hydrogen-bond formation with ACH. Consequently, we concluded that the hydroxyl hydrogen rather than the quinolinic nitrogen in 7HQ plays a major role for the 7HQ/ACH hydrogen-bond formation.

Excited-State Spectroscopy and Dynamics. *7HQ Self-Association*. Table 2 lists the steady-state spectral properties of absorption and emission as well as relaxation dynamics for 7HQ and its hydrogen-bonded species in various nonpolar solvents. When the concentration of 7HQ was prepared as low as 7.0×10^{-6} M in benzene, a weak, normal Stokes shifted emission ($\Phi_f \sim 8.2 \times 10^{-3}$) was observed with a peak maximized at 355 nm. The lifetime was measured to be 0.35 ns and was independent of the excitation as well as the monitored emission wavelength. Therefore, at a sufficiently low concentration of 7HQ in benzene only one emitting species exists in the excited state, which is unambiguously assigned to the enol monomer.

The steady-state fluorescence spectra as a function of the 7HQ concentration are shown in Figure 5. Excitation in the region of 340 nm where 7HQ self-aggregates mainly absorb, dual fluorescence was observed, consisting of a normal Stokes shifted, broad emission band maximum at ~365 nm (the F_1 band) followed by a weak, large Stokes shifted emission maximum at 525 nm (the F_2 band). The excitation spectra monitored at a long-wavelength region of the F_1 band (e.g., 430

TABLE 2: Photophysic Properties of Hydrogen-Bonded Species for 7HQ Derivatives in Various Nonpolar Solvents[a,b]

host	guest	solvents	absorption λ_{max} (nm)	fluorescence λ_{max} (nm)	lifetime τ (ns)
7HQ	7HQ	benzene	332(E)	355(E)	0.35(E)
			340(ED)	365 (ED)	1.2(ED)
				525 (KD)	1.7(KD)
7HQ	ACID	cyclohexane	330(E)	350(E)	0.52(E)
			337(EC)	530(KC)	2.2(KC)
7HQ	ACID	CCl_4	330(E)	352(E)	0.35(E)
			340(EC)	530(KC)	2.0(KC)
7HQ	ACH	cyclohexane	335(EC)	365(EC)	0.52(EC)
7HQ	ACH	CCl_4	335(EC)	(EC)[c]	(EC)[e]
7MQ	ACID	cyclohexane	330(E)	348(E)	0.39(E)
			(EC)[d]	(EC)[c]	(EC)[e]
7MQ	ACID	CCl_4	330(E)	352(E)	0.32(E)
			(EC)[d]	360(EC)	(EC)[e]
7MQ	ACH	cyclohexane	*f*		
7MQ	ACH	CCl_4	*f*		

[a] E, enol monomer; ED, enol dimer; KD, keto dimer; EC, enol complex. [b] The maximum of $S_0 \rightarrow S_1$ transition for the enol monomer was taken from the absorption spectrum, while that of dimer or complex was measured by the excitation spectrum. [c] The emission was too weak to be observed. [d] The excitation spectrum of the complex was not obtainable due to the extremely weak fluorescence. [e] Beyond the response time of the detecting system(~200 ps). [f] No complex formation was observed.

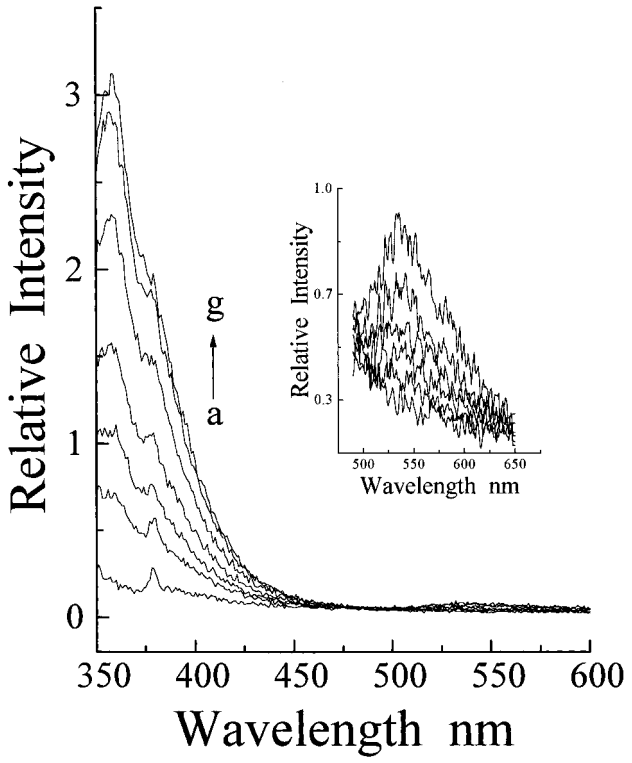

Figure 5. The fluorescence spectra of 7HQ in benzene as a concentration of (a) 7.0×10^{-6}, (b) 2.0×10^{-5}, (c) 4.0×10^{-5}, (d) 6.0×10^{-5}, (e) 1.0×10^{-4}, (f) 1.4×10^{-4}, and (g) 1.8×10^{-4} M ($\lambda_{ex} = 340$ nm). Insert: The magnified view (×30) of the fluorescence spectra in the region of 500−600 nm.

nm) and the F_2 band (e.g., 525 nm) are similar, exhibiting a peak maximum at 340 nm which is ~10 nm red-shifted relative to that of the monomer (see Table 2). Thus, it seems straightforward to ascribe both F_1 and F_2 bands to the 7HQ self-association species of which both excitation and emission spectra are red-shifted with respect to that of the monomer form due to the hydrogen-bond formation. However, detailed time-resolved studies indicate that F_1 and F_2 bands undergo different relaxation dynamics. The decay monitored at the F_1 band was fit poorly

SCHEME 2

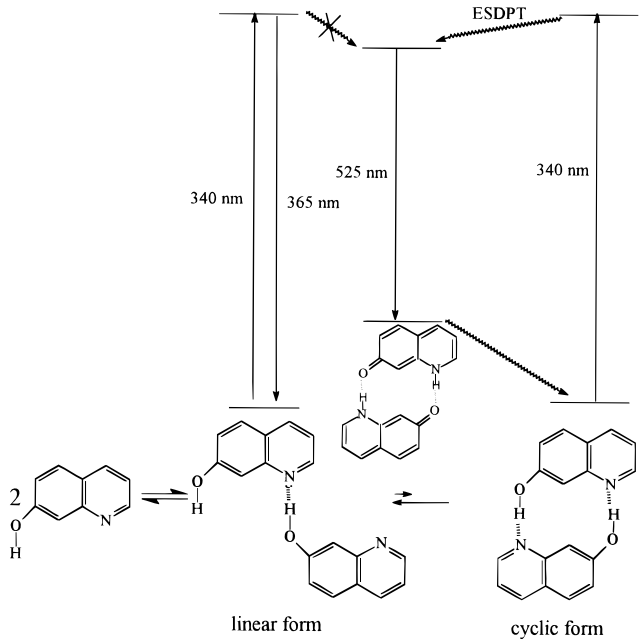

by single exponential decay dynamics. Instead, it is well fit by a double exponential decay which is theoretically expressed as

$$F(t) = A_1 e^{-k_1 t} + A_2 e^{-k_2 t} \quad (6)$$

where A_1 and A_2 are the emission intensity at $t \sim 0$ for the decay components 1 and 2, respectively. Although the ratio for A_1 versus A_2 is concentration as well as excitation-wavelength dependent, k_1 and k_2, within experimental error, were found to be constant, with a fast and a slow component of $(2.8 \pm 0.1) \times 10^9$ s^{-1}($\tau \sim 0.36$ ns) and $(8.3 \pm 0.2) \times 10^8$ s^{-1} ($\tau \sim 1.2$ ns), respectively (see Table 2). Since the rise time for both components cannot be resolved, it is quite unlikely that one species is the precursor of the other. The results indicate the existence of two distinct decay species in the region of the F_1 band. The faster decay one can be reasonably ascribed to the emission from the non-hydrogen-bonded monomer due to its nearly identical decay rate with that of 7HQ in sufficiently low concentration. Accordingly, the longer-lived species is tentatively assigned to a 7HQ associated species (hereafter denoted as the F_1' band), most likely the 7HQ dimeric form concluded in the absorption titration study. On the other hand, it is relatively straightforward to analyze the F_2 band. When the emission was monitored at >520 nm, a wavelength-independent single-exponential decay was observed ($\tau_f \sim 1.7$ ns). Since F'_1 ($\tau = 1.2$ ns) and F_2 ($\tau = 1.7$ ns) bands exhibit different relaxation dynamics and the rise time for each is beyond the response time of our photon counting system (~200 ps), it is very unlikely that both F'_1 and F_2 bands originate from the same type of dimeric form. Due to similar spectral features with the 540 nm keto-tautomer emission in methanol solution and a large Stokes shift of ~10,000 cm^{-1} relative to the dimeric absorption (340 nm, see Table 2), it is thus reasonable to ascribe the F_2 band to the 7HQ keto-tautomer emission. One type of 7HQ dimeric form responsible for the F_2 band plausibly possesses a cyclic hydrogen-bonding configuration (see Scheme 2) where the dual hydrogen-bonding sites, i.e., the hydroxyl proton and the pyridinal nitrogen in 7HQ, act as a proton donor and acceptor, respectively. Thus, the $\pi \rightarrow \pi^*$ excitation resonantly induces an electron charge flow from the hydroxyl oxygen to

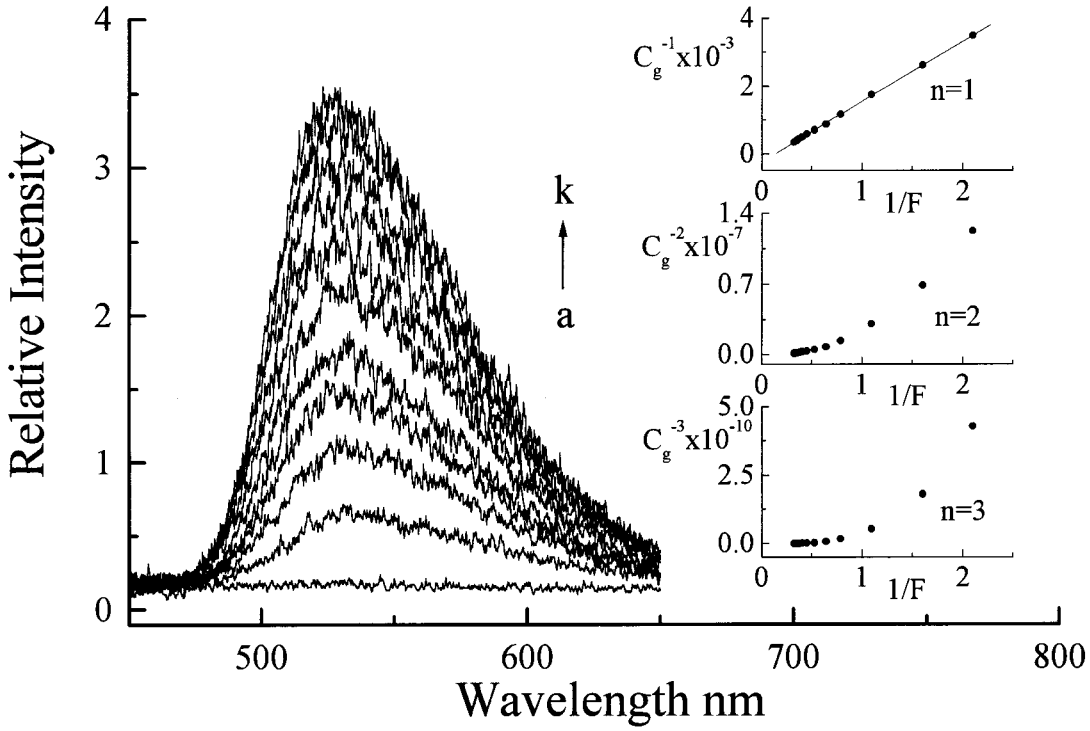

Figure 6. The fluorescence spectra of 7HQ in CCl_4 by adding various ACID concentrations (C_g) of (a) 0, (b) 2.9×10^{-4}, (c) 5.7×10^{-4}, (d) 8.6×10^{-4}, (e) 1.1×10^{-3}, (f) 1.4×10^{-3}, (g) 1.7×10^{-3}, (h) 2.0×10^{-3}, (i) 2.3×10^{-3}, (j) 2.6×10^{-3}, and (k) 2.9×10^{-3} M. Insert: the plot of $1/c_g^n$ against $1/F$ up to $n = 3$.

the pyridinal nitrogen, triggering the double proton-transfer reaction. On the other hand, the existence of a linear 7HQ dimer possessing only a single hydrogen bond (see Scheme 2) is also proposed, in which the ESDPT is prohibited during its excited-state life span due to the requirement of a large proton displacement, resulting in a normal Stokes shifted emission. Since a derivation for the fluorescence intensity (F) based on eq 3 as a function of the added 7HQ concentration involves an instrument factor, it is not possible to extract the K_a value simply by plotting C_0/F versus the square root of $1/F$. This in combination with similar excitation spectra (i.e., the same absorption profile) for both species, making it impossible to obtain the relative population. Alternatively, if we assume the same radiative lifetime, a small difference in the observed decay rates leads to a similar fluorescence quantum yield for both F_1' and F_2 bands. Accordingly, assuming an ultrafast ESFPT in the cyclic form, the relative population between linear and cyclic dimers is equivalent to the intensity ratio for the F_1' versus the F_2 band, which was calculated to be >30, indicating a predominant linear dimeric species existing in the self-association reaction. Further support of this viewpoint as well as detailed discussion regarding thermodynamic properties of these two dimeric species will be given in a later section.

7HQ/guest hydrogen-bonded complexes Figure 6 shows the fluorescence spectra as a function of the added ACID concentration in CCl_4. Upon 350 nm excitation which is mainly attributed to the absorption of 7HQ/ACID hydrogen-bonded complex, only a large Stokes shifted emission maximum at 520 nm (the F_2 band) was observed. The lifetime is independent of the monitored emission wavelength and can be well fit by single-exponential decay dynamics with a decay rate, k_f , of $(4.6 \pm 0.2) \times 10^8$ s^{-1} ($\tau_f \sim 2.2$ ns), indicating the existence of only one emitting species. On the basis of a Benesi−Hildebrand derivation for the fluorescence titration,[19] the relationship between the initially prepared ACID concentration, C_g, and the measured 530 nm emission intensity F can be expressed in eq 6:

$$\frac{1}{C_g^n} = aC_0\epsilon_{350}K_a\frac{1}{F} - K_a \qquad (6)$$

where α is the instrument factor, including sensitivity, alignment, etc., of the detecting system.

For $n = 1$ where 7HQ and ACID are hydrogen-bonded in a 1:1 ratio, the plot of $1/C_g$ versus the inverse of the integrated 530 nm emission band, $1/F_{530}$ shows very good linear behavior, whereas significant deviation from the linear behavior was observed when plotting $1/C_g^n$ versus $1/F_{530}$ for $n \geq 2$ (see insert of Figure 6). The results are consistent with the absorption titration study, concluding that the 1:1 7HQ/ACID complex is a predominantly hydrogen-bonded species existing in equilibrium. For the $n = 1$ plot, an intercept of the best least-squares fit gives a K_a value of $(3.3 \pm 0.1) \times 10^2$ M^{-1} in CCl_4, consistent with that obtained from the absorption titration study. More importantly, the results clearly indicate that the precursor for the 530 nm emission originates from a 1:1 7HQ/ACID hydrogen-bonded species. The unusually large Stokes' shifted emission (~10 000 cm^{-1} peak-to-peak between absorption and emission maxima) may be rationalized by two possible photophysical processes. On one hand, since the basicity of the quinolinic nitrogen on 7HQ increases drastically in the excited state (ΔpK_a (NH^+) = pK_a (NH^+) − pK_a* (NH^+) = −7.86),[8] the observed 530 nm band may simply result from the excited-state adiabatic proton transfer from the carboxylic proton to the 7HQ quinolinic nitrogen, giving rise to a cationic type of 7HQ emission. To examine such a possibility 7MQ was used as a prototype. It has been concluded in the absorption titration experiment that the formation of a 7MQ/ACID complex, similar to the 7HQ/ACID hydrogen-bonding site, incorporates the quinolinic nitrogen of 7MQ and carboxylic proton of acetic acid.

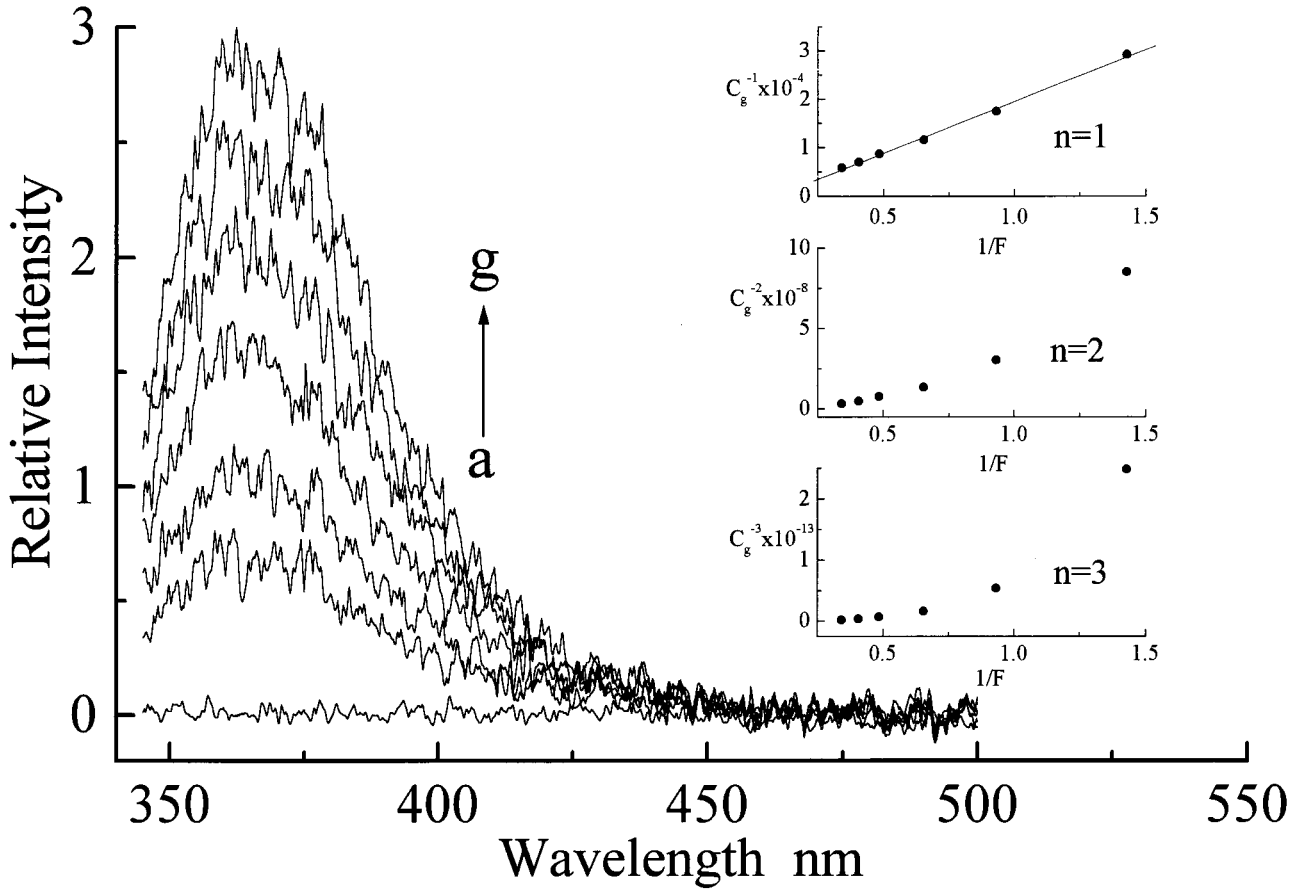

Figure 7. The concentration-dependent emission spectra of 7HQ in cyclohexane by adding various ACH concentrations (C_g) of (a) 0, (b) 3.4×10^{-5}, (c) 5.7×10^{-5}, (d) 8.6×10^{-5}, (e) 1.1×10^{-4}, (f) 1.4×10^{-4}, and (g) 1.7×10^{-4} M.

Upon excitation the 7MQ/ACID complex exhibits a weak emission band maximum at 360 nm ($\Phi_f = 8.2 \times 10^{-4}$) which is unambiguously assigned to the 7MQ/ACID normal Stokes shifted emission. Since a pK_a* of 13.2 for 7MQ(NH^+) measured by a fluorescence titration is comparable to that of 7HQ(NH^+) (pK_a* = 13.5[8]), similar photophysical properties, i.e., the excited-state protonation if there is any, should be expected. In contrast, the lack of observing any large Stokes shifted emission in the 7MQ/ACID complex discounts the assignment of the 530 nm emission simply to the excited-state protonation of 7HQ. Alternatively, the same spectral features as the keto-tautomer emission in the methanol solution lead us to conclude the occurrence of the excited-state double proton transfer (ESDPT) in the 7HQ/ACID complex, resulting in a keto-tautomer emission. Mechanistic details regarding the proton-transfer dynamics will be elaborated in the discussion section.

The formation of a 1:1 7HQ/ACH hydrogen-bonded complex has also been verified in the absorption titration study. Since ACH also possesses bifunctional hydrogen-bonding groups, it is reasonable to expect the 7HQ/ACH complex to exhibit the same photophysical properties, i.e., the ESDPT, as that of 7HQ/ACID. Note that for the cases of 3HIQ and 7AI both 3HIQ/ACID and 3HIQ/ACH complexes (or 7AI/ACID and 7AI/ACH complexes) undergo similar ESDPT dynamics.[1−4] However, in contrast, increasing the ACH concentration results in an increase of the emission intensity maximum at 365 nm (see Figure 7). While within the detection limit, the tautomer emission expected to be in the region of 500−600 nm was not observed. The prohibition of ESDPT in the 7HQ/ACH complex suggests that 7HQ/ACID and 7HQ/ACH undergo drastically different relaxation dynamics in the excited state, possibly due to their different hydrogen-bonding configurations concluded in the earlier absorption titration experiment. A detailed explanation will appear in the following section.

Discussion

Hydrogen-Bonding Formation. In the study of 7HQ self-association we have concluded the existence of two types of dimeric forms in the ground-state equilibrium, namely the cyclic and linear dimers. However, it is intriguing to know why the linear form possessing only a single hydrogen bond is a dominant dimeric species rather than that of the cyclic dimeric form incorporating the CDHB formation. To rationalize this result, we have performed an ab initio calculation for the 7HQ self-association in various hydrogen-bonding configurations. Figure 8b and c depict the full geometry optimized structures (6-31G(d,p) basis set) of 7HQ cyclic and linear dimeric forms. For the case of the cyclic dual hydrogen-bonded dimer, the association enthalpy, ΔH_{ac}, was calculated to be −6.39 kcal/mol, which is surprisingly 0.67 kcal/mol less exothermic than that of the linear dimer ($\Delta H_{ac} = -7.06$ kcal/mol, see Table 3). In comparison to other CDHB complexes such as the 3HIQ dimer[4] where the type of dual hydrogen bonds as well as the associated resonance effect are similar to that of the 7HQ CDHB dimer, ΔH_{ac} is calculated to be −10.2 kcal/mol. For the case of the 7AI CDHB dimer ΔH_{ac} was calculated to be as large as −11.3 kcal/mol.[20] These results clearly indicate that in addition to the CDHB effect which introduces great stabilization, other factors may play an important role to reversibly destabilize the 7HQ cyclic dimer formation. Further structural analysis reveals that in a geometry optimized 7HQ cyclic dimer, the distance between two hydrogen atoms at the 8th carbon atom is as close

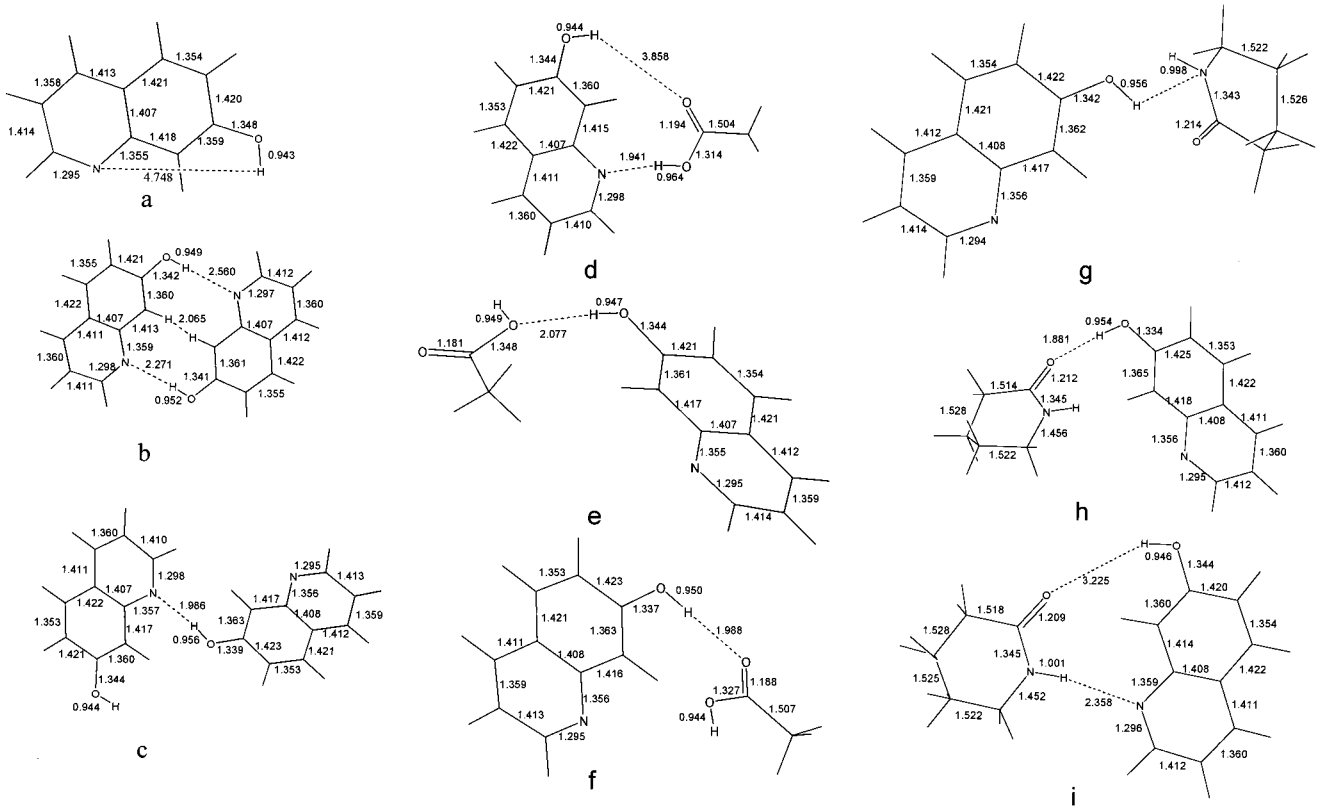

Figure 8. Optimized geometries based on the HF/6-31G(d,p) basis set (in Å and degrees, only critical angles are shown) for the ground states of (a) 7HQ monomer, (b) cyclic dimer, (c) linear dimer, (d) 7HQ(−N−)/ACID(−OH), (e) 7HQ(−OH)/ACID(−O−), (f) 7HQ(−OH)/ACID(═O), (g) 7HQ(−OH)/ACH(−N−), (h) 7HQ(−OH)/ACH(═O), and (i) 7HQ(−N−)/ACH(−NH).

TABLE 3: Thermodynamic Properties of 7HQ and Its Hydrogen-Bonded Species in the Gas Phase Calculated by the RHF/6-31G(d,p) Basis Set at 298 K[a]

	total *E*	ZPE	*H*(scaled)	*G*(scaled)	$\Delta H°$	$\Delta G°$
7HQ	−474.22414	0.15028	−474.07794	−474.11830	0	0
ACID	−227.82217	0.06672	−227.75561	−227.78773	0	0
ACH	−323.93247	0.15042	−323.78739	−323.82447	0	0
cyclic dimer	−948.46030	0.30262	−948.16605	−948.22786	−6.39	5.48
linear dimer	−948.46211	0.30232	−948.16713	−948.23370	−7.06	1.82
7HQ(−N−)/ACID(−OH)	−702.06332	0.21888	−701.84813	−701.90496	−9.15	0.68
7HQ(−OH)/ACID(−O−)	−702.05342	0.21836	−701.83845	−701.89771	−3.08	5.22
7HQ(−OH)/ACID(═O)	−702.04685	0.21808	−701.83504	−701.89575	−5.84	2.40
7HQ(−OH)/ACH(−N−)	−798.17353	0.30282	−797.87957	−797.94219	−8.94	0.36
7HQ(−OH)/ACH(═O)	−798.17273	0.30255	−797.87891	−797.94182	−8.52	0.60
7HQ(−N−)/ACH(−NH)	−798.16958	0.30233	−797.87418	−797.93722	−5.55	3.48

[a] Total energy, enthalpy, and free energy in hartrees. [b] $\Delta H°$ and $\Delta G°$ (in kcal/mol) values for various hydrogen-bonded species were calculated relative to 7HQ and the associated guest molecule.

as 2.065 Å ((see Figure 8b). Such a configuration is expected to significantly increase a repulsion energy which may compensate the energy stabilized by the CDHB effect. It should be noted that similar close-packed interference between two hydrogen atoms does not exist in the 3HIQ and 7AI CDHB dimers because the proton donor and acceptor are either adjacent to each other in 3HIQ or separated by a fused carbon atom in 7AI. Perhaps the strongest support for this viewpoint regarding a steric effect was given by the study of 8MHQ self-association in which a concentration-dependent absorption spectrum was not observed up to 1.0×10^{-3} M in benzene. In addition, the keto-tautomer emission cannot be resolved under our detection limit. The lack of observation of 8MHQ keto emission indicates a negligible population of the CDHB dimeric form, a precursor for the ESDPT reaction, in the ground-state equilibrium. The result is also consistent with an ab initio calculation where an attempt to obtain an geometry optimized 8MHQ CDHB dimeric form failed, possibly due to the build-up of an enormous repulsion energy between two 8-methyl groups when 8MHQ molecules approach each other in a C_{2v} symmetry. Interestingly, although a stable 8MHQ linear form was obtained through a full geometry optimization, the association enthalpy was calculated to be as small as −1.5 kcal/mol, indicating that the methyl function group at the 8th position may also induce a certain degree of steric hindrance even for the linear dimeric form, rationalizing the failure in detecting any 8MHQ self-association in the absorption titration study. Finally, due to its lower formation enthalpy in combination with a more favorable entropy factor, the formation free energy for the linear form was calculated to be more exergonic than that of the of the cyclic dimer by 3.7 kcal/mol. The results are qualitatively consistent with the experimental observation, concluding that the linear dimeric is a dominant species in the self-association reaction.

For those 7HQ/guest hydrogen-bonded complexes our results show that independent of the type of guest molecule studied, the formation of a 7HQ/guest complex generally incorporates

TABLE 4: pK_a Values for Various Functional Groups in 7HQ, 7MQ, and Guest Molecules

	7HQ(−NH$^+$)	7HQ(O−H)	7MQ(−NH$^+$)	ACID(−OH)	ACID(=OH$^+$)	ACID (OH_2^+)	ACH(NH_2^+)	ACH(−NH)	ACH(=OH$^+$)
pK_a[a]	5.64[a]	8.67[a]	5.04[b]	4.75[c]	−6.5[c]	<−6.5[d]	−1[c]	26.5[c]	−0.5[c]

[a] Mason, S. F. *J. Chem. Soc.* **1958**, 674. [b] Data was obtained in this work. [c] Gordon, Arnold J.; Ford, R. A. *The Chemist's Companion*; John Wiley & Sons: New York, 1972. [d] Not available due to its stronger acidity than ACID(=OH$^+$).

a single hydrogen bond. This can be rationalized by the large separation between the proton donor (the hydroxyl proton) and acceptor (the quinolinic nitrogen) of 4.748 Å in 7HQ (see Figure 8a). In an earlier section, the application of 7MQ, 8MHQ, and guest molecules possessing different hydrogen-bonding functionality has led us to distinguish the active functional group involved in the hydrogen-bonding formation. In this section, we further carried out a theoretical approach in order to verify the experimental results. Table 3 lists the calculated formation of enthalpy, entropy, and consequently the free energy among those geometry-optimized hydrogen-bonded complexes. For the 1:1 7HQ/ACID complex, three possible geometry optimized structures were resolved and depicted in Figure 8d−f. The calculated ΔH_{ac} of −9.15 kcal/mol for the 1:1 7HQ(−N−)/ACID(−OH) complex (denoting a hydrogen-bond formation between the pyridinal nitrogen in 7HQ and the carboxylic proton in acetic acid) is more exothermic than those of 7HQ(−OH)/ACID(−O−) and 7HQ(−OH)/ACID(=O) and by 6.07 and 3.31 kcal/mol, respectively, and is concluded to be the most stable form according to its lowest formation free energy (see Table 3). We also performed a full geometry optimization of a 1:2 7HQ/$(ACID)_2$ complex, and ΔH_{ac} was estimated to be −12.7 kcal/mol. Such a large stabilization energy can be rationalized by a dual hydrogen-bond formation. However, the requirement of two ACID molecules in a specific hydrogen-bonding configuration significantly decreases the formation entropy. As a result, the formation free energy was calculated to be 3.5 kcal/mol more endergonic than that of the 1:1 7HQ(−N−)/ACID(−OH) complex, consistent with the experimental result where the 1:1 7HQ(−N−)/ACID(−OH) complex is the predominant hydrogen-bonded species at ambient temperature.

On the other hand, the geometry optimized 1:1 7HQ/ACH complex in its most stable form is drastically different from that of the 7HQ/ACID. Surprisingly, the quinolinic nitrogen acting as a proton acceptor in the self-dimerization and the formation of a 7HQ/ACID complex is no longer the most stable hydrogen-bonding site in the case of 7HQ/ACH complex. Instead, the 1:1 7HQ(−OH)/ACH(−N−) and 7HQ(−OH)/ACH(=O) hydrogen-bonded complexes(see Figure 8g,h) were calculated to be more exothermic than 7HQ(−N-)/ACH(−NH) by 3.4 and 2.8 kcal/mol, respectively (see Table 3). Due to their similar formation entropy, 7HQ(−OH)/ACH(−N−) and 7HQ(−OH)/ACH(=O) complexes were consequently calculated to be the most stable conformers and should be the predominant hydrogen-bonded species in the solution. The result is consistent with the absorption titration study, concluding the hydroxyl proton in 7HQ to be the active hydrogen-bonding site in the formation of a 7HQ/ACH complex.

Table 4 summarizes pK_a values of various hydrogen-bonding sites for both host and guest molecules. Although these data are obtained in the aqueous solution, an interesting correlation was observed between the sum of pK_a (proton donor) and pK_b (proton acceptor, $pK_b = pK_{H_2O} - pK_a$, where K_{H_2O} is the autoprotolysis constant of H_2O) and the hydrogen-bonding site actively involved in the complex formation. For instance, in the case of a 1:1 7HQ/ACID complex, the value of $pK_a + pK_b$ was calculated to be on the order of 7HQ(−N−)/ACID(−OH) ≪ 7HQ(−OH)/ACID(−O−) ∼ 7HQ(−OH)/ACID(=O), which correlates well with the experimental as well as ab initio result of the 7HQ(−N−)/ACID(−OH) form being the most stable complex in the equilibrium. In contrast, for the case of 7HQ/ACH, the sum of pK_a and pK_b for 7HQ(−OH)/ACH(−N−) and 7HQ(−OH)/ACH(=O) complexes turns out to be smaller than that of the 7HQ(−N−)/ACH(−NH) complex by a factor of 10, again corresponding to the trend of the stability obtained experimentally as well as predicted by the ab initio approach. Since the difference in the entropy of formation is negligibly small among those 1:1 7HQ/guest complexes at 298 K, the equilibrium for the complexation is mainly tuned by the association enthalpy, i.e., the hydrogen-bonding strength. Consequently, a correlation between the hydrogen-bonding strength and their corresponding acid and base properties may be established. The sum of pK_a and pK_b is equivalent to $-\log K_{eq}$ where K_{eq} denotes an equilibrium constant for the acid−base reaction. Hence, a lower $pK_a + pK_b$ value indicates a large acid−base equilibrium constant, and the reaction favors the product formation. Empirically, the more exergonic the acid−base reaction, the lower the free energy of formation of the activated complex. If the hydrogen-bonded species can be reasonably assumed to be an activated complex-like species during the acid−base reaction, a larger value of K_{eq} may simply indicate the formation of a more stable hydrogen-bonded complex, consistent with both experimental and theoretical results. However, it should be noted that such a conclusion is qualitative since the hydrogen-bonded complex is in its local minimum energy and hence cannot be simply treated as an activated complex. In addition, the correlation was made where the difference in $pK_a + pK_b$ between various hydrogen-bonding configurations is generally quite large (normally ≫ 5). Once the difference becomes small the correlation may be discounted due to an uncertainty by applying the pK_a (or pK_b) value obtained in the aqueous solution to a nonpolar (or gas) environment. Finally, when the proton affinity between donor and acceptor is close enough, the formation of an unusually strong hydrogen bond has been reported in several enzymatic reactions and subsequently verified by theoretical approaches,[21−23] for which the aforementioned empirical correlation may no longer be valid. Fortunately, the proton affinity for each of various functional groups applied in the case of the 7HQ hydrogen-bonded complex is substantially different from the others, excluding the possibility of an unusually strong hydrogen-bonding formation.

Proton-Transfer Dynamics. In the cases of 7AI/ACID and 3HIQ/ACID CDHB complexes where dual hydrogen bonds are intrinsically formed, the double proton transfer in the excited state only requires a small displacement of the hydrogen atom and/or molecular skeleton. The rate of such a cooperative proton-transfer reaction, either taking place stepwise or simultaneously, should be fast and perhaps mainly dominated by the tunneling mechanism. In comparison, the occurrence of the ESDPT in the single hydrogen-bonded 7HQ/ACID system is intriguing from the viewpoint of the proton-transfer dynamics. For the case of 7HQ(−N−)/ACID(−OH) complex, the ESDPT requires a transfer of proton from the carboxylic site to the quinolinic nitrogen through the existing hydrogen bond followed by a transfer of the hydroxyl proton in 7HQ(−OH) to the carbonyl

SCHEME 3

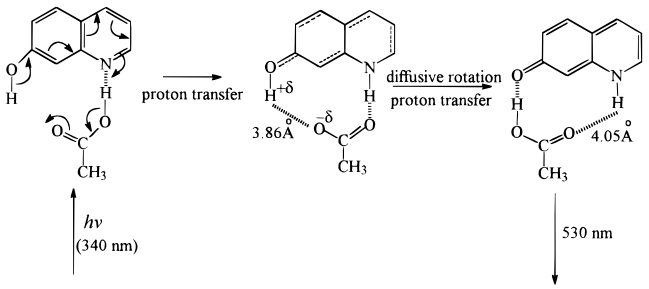

oxygen of ACID(═O). However, a full geometry optimized structure of the 7HQ(−N−)/ACID(−OH) complex clearly shows that the hydroxyl proton in 7HQ and carbonyl oxygen in ACID are far separated from each other by 3.858 Å. The lack of hydrogen-bond formation in combination with a large hydrogen displacement may significantly reduce the proton tunneling rate, hence prohibiting the ESDPT within the life span of the excited 7HQ(−N−)/ACID(−OH) complex. In contrast, the observation of a predominant keto emission with an instrument-response limited rise time ($>5 \times 10^9$ s^{-1}) indicates that the rate of ESDPT must be still rapid in comparison to other relaxation processes. Upon deuteration on both 7HQ and ACID, no isotope effect was observed with respect to the decay rate, as well as the tautomer emission intensity. In addition, the rise time was still beyond the response of our photon counting system ($\sim$ 200 ps). The lack of isotope effect for the proton-transfer emission implies that high-frequency O−H or N−H vibrations may not serve as main energy acceptors. Alternatively, radiationless quenching by small-frequency vibrational modes associated with the intermolecular hydrogen-bonding interaction, i.e., the hydrogen-bonding strength, may play a key role to account for the small keto-tautomer emission yield. To rationalize the results discussed in this section we tentatively propose a proton-transfer mechanism depicted in Scheme 3 where the π-electron excitation of the 7HQ(−N−)/ACID(−OH) complex induces a charge redistribution of 7HQ, resulting in a drastic increase of the acidity and basicity for the hydroxyl proton ($pK_a^* \sim -2.7$) and quinolinic nitrogen ($pK_a^* \sim 13.3$), respectively. Subsequently, an triggering step for the ESDPT may incorporate the proton transfer through a preexisting 7HQ-(−N−)/ACID(−OH) hydrogen bond, which leads to an increase of the basicity, i.e., a build-up of partial negative charge density, at the carbonyl oxygen site of ACID. This in combination with the partial positive charge of the hydroxyl proton creates an electrostatic attraction which acts as a driving force for the adjustment (or displacement) of both 7HQ and ACID to a right conformation so that the second-step proton transfer can take place through a lowest potential energy surface. For this case, acetic acid acts as a proton donor and acceptor simultaneously to achieve an autocatalytic process where the overall proton-transfer rate may be correlated with the rotational diffusion dynamics of 7HQ and/or ACID in solution. On the other hand, for 7HQ(−OH)/ACH(−N−) and 7HQ(−OH)/ACH(═O) complexes where the amino proton in ACH and the pyridinal nitrogen in 7HQ are far separated by 6.04 and 4.25 Å, respectively, the induction effect, a driving force proposed to induce the rotational diffusion, will be drastically reduced. In addition, neither the carbonyl site ($pK_a \sim 0.5$) nor the nitrogen site ($pK_a \sim -1.0$) in ACH is a good proton acceptor for the first-step proton-transfer reaction. Both factors may play important roles to rationalize the experimental result where ESDPT was prohibited in the 7HQ/ACH complex. Further study focusing on the 7HQ proton-transfer dynamics in the pico-femtosecond region should be performed to verify the proposed mechanism.

Conclusion

We have studied hydrogen-bonded complexes of 7HQ by means of absorption, emission, and ab initio approaches. A specific hydrogen-bonding site in the complex has been determined by applying various derivatives of 7HQ incorporated with guest molecules possessing only either a proton-donating or -accepting site. The result was rationalized by a correlation of the hydrogen-bond strength with respect to the donor's acidity and the acceptor's basicity. For self-association, there exists an equilibrium with similar association constants for both 7HQ cyclic and linear dimers at room temperature. The 7HQ cyclic dimer undergoes fast ESDPT, resulting in a unique keto-tautomer emission. For the case of 1:1 7HQ/ACID complex possessing only a single hydrogen bond, the ESDPT reaction also takes place, forming a keto/ACID complex. The result can be tentatively rationalized by a mechanism incorporating both proton transfer and rotational diffusion dynamics depicted in Scheme 3.

Acknowledgment. Start-up support from the National Chung-Cheng University is graciously acknowledged. This work was supported by the National Science Council, Taiwan, R.O.C. (Grant NSC 87 -2119-M-194-002). We thank the National Center for High-Performance Computing, Taiwan, for the use of their facility. We also thank Professor Shannon Martinez for many helpful discussions.

References and Notes

(1) Chang, C. P.; Hwang, W. C.; Kuo, M. S.; Chou, P. T.; Clements, J. H. *J. Phys. Chem.* **1994**, *98*, 8801.
(2) Chou, P. T.; Wei, C. Y.; Chang, C. P.; Kuo, M. S. *J. Phys. Chem.* **1995**, *99*, 11994.
(3) Chou, P. T.; Wei, C. Y.; Hung, F. T. *J. Phys. Chem.* **1997**, *101*, 9119.
(4) Wei, C. Y.; Yu, W. S.; Chou, P. T.; Hung, F. T.; Lin, T. C.; Chang, C. P. *J. Phys. Chem.* **1998**, *102B*, 1053.
(5) Ingham, K. C.; El-Bayoumi, M. A. *J. Am. Chem. Soc.* **1971**, *93*, 5023.
(6) Ingham, K. C.; El-Bayoumi, M. A. *J. Am. Chem. Soc.* **1974**, *96*, 1674.
(7) Douhal, A.; Kim, S. K.; Zewail, A. H. *Nature* **1995**, *378*, 260.
(8) Mason, S. F.; Philip, J.; Smith, B. E. *J. Chem. Soc. A* **1968**, 3051.
(9) Thistlethwaite, P. J.; Corkill, P. J. *Chem. Phys. Lett.* **1982**, *85*, 317.
(10) Thistlethwaite, P. J. *Chem. Phys. Lett.* **1983**, *96*, 509.
(11) Itoh, M.; Adachi, T.; Tokumura, K. *J. Am. Chem. Soc.* **1984**, *106*, 850.
(12) Konijnenberg, J.; Ekelmans, G. B.; Huizer, A. H.; Varma, C. A. G. O. *J. Chem. Soc., Faraday Trans. 2* **1989**, *85*, 39.
(13) Bohra. A.; Lavin, A.; Collins, S. *J. Phys. Chem.* **1994**, *98*, 11424.
(14) Nakagawa, T.; Kohtani, S.; Itoh, M. *J. Am. Chem. Soc.* **1995**, *117*, 7952.
(15) Vogel, A. I.; Furniss, B. S.; Hannaford, A. J.; Rogers, V.; Smith, P. W. G.; Tatchell, A. R. *Vogel's Textbook of Practical Organic Chemistry*; Wiley: New York, 1989.
(16) Demas, J. N.; Crosby, G. A. *J. Phys. Chem.* **1971**, *75*, 991−1024.
(17) (a) Wang, J.; Boyd. R. J. *Chem. Phys. Lett.* **1996**, *259*, 647. (b) Wang, J.; Boyd, R. J. *J. Phys. Chem.* **1996**, *100*, 16141.
(18) Wong, M. W.; Wiberg, K. B.; Frisch, M. J. *J. Am. Chem. Soc.* **1992**, *114*, 1645.
(19) Benesi, M. L.; Hildebrand, J. H. *J. Am. Chem. Soc.* **1949**, *71*, 2703.
(20) Note that these values were obtained without applying a counterpoise correction due to the basis-set superposition (BSSE). In many cases, we have found that ΔH_{ac} obtained experimentally in nonpolar solvents is even closer to the result (in the gas phase) without a counterpoise correction. Therefore, for a qualitative comparison using a relative ΔH_{ac} in this study, the method invoking counterpoise correction was skipped.
(21) Gerlt, J. A.; Gassman, P. G. *J. Am. Chem. Soc.* **1993**, *115*, 11552.
(22) Cleland, W. W.; Kreevoy, M. M. *Science* **1994**, *264*, 1887.
(23) Frey, P. A.; Whitt, S. A.; Tobin, J. B. *Science* **1994**, *264*, 1927.